Journal of Science and Technology – Smart Systems and Devices
Volume 36, Issue 3, Sep 2026, 000–000

Fast and Accurate Design of Single-Phase Transformers Using Bayesian Neural Networks

Son T. Nguyen*, Tu M. Pham, Anh Hoang, Hung T. Nguyen
Hanoi University of Science and Technology, Hanoi, Vietnam
* *Corresponding author email: son.nguyenthanh@hust.edu.vn*

Abstract

The accurate design of single-phase transformers is essential for achieving high efficiency, reliability, and cost-effectiveness in power applications. However, traditional analytical approaches often depend on simplifying assumptions that limit precision, particularly when estimating core losses and leakage flux. This study introduces a Bayesian Neural Network (BNN)–based method for the precise design of small single-phase power transformers. The Finite Element Method (FEM) is used to generate detailed electromagnetic and performance data under various operating conditions, forming the training dataset for the BNN model. The trained BNN effectively captures complex nonlinear relationships between design parameters and performance indices, enabling fast and accurate prediction of transformer characteristics without repeated FEM simulations. The proposed approach significantly reduces design time, enhances prediction accuracy, and minimizes dependence on empirical trial-and-error techniques. Additionally, an experimental setup is developed to determine the operating point of an existing single-phase transformer, which is subsequently redesigned using the BNN methodology. This study provides a reliable and efficient framework for academic research and education in applying machine learning (ML), including artificial neural networks (ANNs), to the accurate design of electrical equipment.

Keywords: Bayesian neural networks, finite element method, single-phase transformers.

1. Introduction

A single-phase transformer is an electrical device that transfers energy between two circuits based on the principle of electromagnetic induction. It plays a vital role in power systems, serving as one of the most fundamental components for voltage regulation and energy distribution. Single-phase transformers are widely used in residential, commercial, and small industrial settings where single-phase alternating current (AC) power is commonly available. They enable efficient voltage conversion-either stepping up or stepping down-to meet the specific requirements of electrical equipment and power networks while minimizing energy losses. Due to their simplicity, reliability, and ease of installation, these transformers remain indispensable in everyday power distribution systems [1, 2].

Designing a single-phase transformer involves selecting appropriate core dimensions, the number of turns, wire sizes, and materials to satisfy specified electrical requirements such as rated voltage, current, requency, efficiency, and voltage regulation.Traditionally, transformer design relies on empirical formulas, magnetic circuit theory, and practical engineering experience to determine dimensions, material selections, and performance characteristics [3, 4]. The primary advantages of this approach are its simplicity and minimal dependence on computational tools, making it particularly suitable for small-and medium-sized transformer design. However, the traditional method has notable limitations, including reduced accuracy in optimizing core geometry and the inability to fully account for leakage flux effects.

Finite Element Analysis (FEA) has been widely used to simulate and optimize the electromagnetic, thermal, and mechanical behavior of transformers prior to physical prototyping [5-7]. For single-phase transformers, FEA enables accurate prediction of magnetic flux distribution and core saturation, estimation of leakage flux, leakage inductance, and short-circuit reactance, as well as evaluation of core losses-including hysteresis and eddy current losses-under both sinusoidal and non-sinusoidal excitation. In addition, FEA can be applied to analyze temperature rise and thermal stresses in the core and windings, and to investigate mechanical deformation, vibration, and acoustic noise. These capabilities support optimal transformer performance, efficiency, and reliability.

Accurate parameter estimation is essential in the design of single-phase transformers, as it directly influences performance, efficiency, and reliability. Key parameters-such as winding resistance, leakage reactance, magnetizing inductance, and core loss components-govern voltage regulation, efficiency, and thermal behavior. In traditional design methods, many of these parameters are calculated using empirical

p-ISSN 3093-3285
e-ISSN 3093-3315
https://doi.org/10.51316/jst.xxx.ssad.2026.36.3.x
Received: Dec 15, 2025; Revised: Feb 22, 2026;
Accepted: Mar 11, 2026; Online: May 29, 2026

In Press

formulas and material data, which may not fully represent real operating conditions. Therefore, precise estimation using experimental measurements [8, 9] or computational techniques such as finite element analysis and optimization algorithms [10, 11] is necessary to bridge the gap between theoretical design and practical performance.

Machine learning (ML) has emerged as a powerful and increasingly essential tool for the modern design and optimization of electrical equipment, including transformers, motors, generators, power converters, and protection systems. By analysing large datasets obtained from experiments, simulations, and operational measurements, ML models can accurately predict system performance, identify meaningful patterns, and optimize critical design parameters. This capability not only enhances design accuracy and efficiency but also significantly reduces development time and cost [12, 13]. Furthermore, ML techniques can adapt to complex, nonlinear behaviours and operating conditions that are difficult to model using conventional analytical methods, making them particularly valuable for improving reliability, efficiency, and overall performance in advanced electrical systems.

Bayesian Neural Networks (BNNs) are an advanced form of feedforward neural network (FNN) that incorporate Bayesian inference into the learning process to quantify uncertainty in both model parameters and predictions [14]. Unlike conventional neural networks, which produce deterministic outputs, BNNs represent weights and biases as probability distributions rather than fixed values. This probabilistic formulation enables the model to capture both epistemic (model-related) and aleatoric (data-related) uncertainties, resulting in more robust and interpretable predictions. Furthermore, by incorporating prior knowledge during training, BNNs can effectively mitigate overfitting, especially when training data are limited or noisy.

This paper presents an accurate and efficient method for designing single-phase transformers by integrating (BNNs) with data generated from Finite Element Analysis (FEA). By leveraging the predictive capability of BNNs, the proposed approach greatly reduces the need for extensive manual design iterations and offers a practical tool for determining optimal transformer design parameters. The effectiveness of the method is validated through both simulation and experimental results, demonstrating strong robustness and generalization across transformers with different ratings and specifications. The main contributions of this work are: (1) the development of a Bayesian Neural Network (BNN)-based framework capable of accurately mapping electrical performance parameters to design parameters, and (2) the incorporation of FEA-generated datasets to enhance prediction accuracy and ensure that the designed transformers meet real-world performance requirements. This integrated approach not only streamlines the design workflow but also improves reliability, efficiency, and scalability in transformer design.

The paper is organized as follows. Section 2 presents the determination of the geometrical parameters of a single-phase transformer. Section 3 describes the equivalent circuits of single-phase transformers, which are essential for determining the operating points of existing or prototype transformers. Section 4 details the development of a BNN for mapping electrical parameters to transformer design parameters. Section 5 provides a brief introduction to the Nelder-Mead method, which is used to extract the parameters of the exact equivalent circuit. Section 6 outlines the key steps involved in designing single-phase transformers using BNNs. Section 7 presents the experimental validation of the proposed method. Finally, Section 8 concludes the paper.

2. Geometrical Parameters of Single-Phase Transformers

The design of a single-phase transformer involves the systematic determination of its fundamental geometrical parameters, which are critical to ensuring optimal electrical and magnetic performance. These parameters include the core dimensions-such as the core cross-sectional area, tongue width, window height, and window width-as well as the number of turns in both the primary and secondary windings. These design variables directly affect the transformer's voltage transformation ratio, efficiency, and thermal performance.

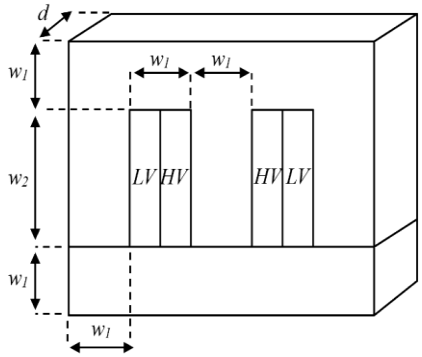

Fig. 1. Basic geometrical dimensions of an EI-core single-phase transformer

Fig. 1 illustrates the basic structural dimensions of an EI-type core commonly used in single-phase transformer construction. These dimensions serve as references for standard design calculations and finite element modelling. To reduce the number of design variables, only three fundamental core dimensions are considered: the tongue width (w_1), the window height (w_2) and the core depth (d). The remaining dimensions can be derived from these three primary parameters. The high-voltage (HV) winding is wound directly around the transformer core column. Surrounding the HV winding, the low-voltage (LV) winding is wound concentrically, separated by

In press

appropriate insulation to ensure electrical safety and reduce leakage flux. This arrangement helps improve magnetic coupling between the windings while maintaining electrical isolation.

The core cross-sectional area can be approximately determined as follows:

$$A_c = K\sqrt{P} \tag{1}$$

Where:

- P : Rated power (W)
- K : A constant between 1.1 and 1.3
- A_c : Core cross-sectional area (cm^2)

According to Fig. 1, the core cross-sectional area can also be expressed as:

$$A_c = w_1.d \tag{2}$$

If the value of w_1 is known, then d can be determined by using (2).

The number of turns per volt can be calculated as follows:

$$TPV = \frac{1}{4.44.f.B_{\max}.A_c} \tag{3}$$

Where:

- TPV : Number of turns per volt
- f : Frequency (Hz)
- B_m : Maximum flux density (T)

The number of turns in the primary winding is computed as follows:

$$N_1 = V_1.TPV \tag{4}$$

Where:

- N_1 : Number of turns in the primary winding
- V_1 : Primary voltage (V)

Similarly, the number of turns in the secondary winding is calculated as follows:

$$N_2 = V_2.TPV \tag{5}$$

Where:

- N_2 : Number of turns in the secondary winding
- V_2 : Secondary voltage (V)

For each winding, the required copper conductor cross-sectional area can be estimated by using the following formula:

$$A_{cu} = \frac{I}{J} \tag{6}$$

Where:

- A_{cu} : Copper conductor cross-sectional area (mm^2)
- I : RMS current through the winding (A)
- J : Current density (A/mm^2)

Typically, $J = 2.5 \div 3.5\left(A/mm^2\right)$ for power transformers with natural cooling. For small or forced-air-cooled transformers, $J = 4 \div 6\left(A/mm^2\right)$.

The area of the window, A_w, can be calculated as follows:

$$A_w = w_1.w_2 \tag{7}$$

The total copper area inside the window is calculated as follows:

$$A_{cu,total} = k_w.A_w \tag{8}$$

Where:

- $A_{cu,total}$: The total copper area (mm^2)
- k_w : The fill factor (usually 0.2 to 0.4)

If the copper areas of the two windings are assumed to be identical, then the copper area for each winding is given by:

$$A_{cu,HV} = A_{cu,LV} = \frac{1}{2}A_{cu,total} \tag{9}$$

The copper conductor cross-sectional area of the primary winding is computed as follows:

$$A_{w1} = \frac{A_{cu,HV}}{N_1} \tag{10}$$

Similarly, the copper conductor cross-sectional area of the secondary winding is computed as follows:

$$A_{w2} = \frac{A_{cu,LV}}{N_2} \tag{11}$$

3. Steady-State Equivalent Circuits of Single-Phase Transformers

Steady-state equivalent circuits of single-phase transformers can be classified into two types:

- Exact steady-state equivalent circuit,
- Approximate steady-state equivalent circuit.

The exact steady-state equivalent circuit of single-phase transformers is depicted in Fig. 2. This model represents the transformer with all of its electrical elements placed in their true physical positions. It includes the primary and secondary winding resistances, leakage reactances, magnetizing reactance, and core-loss resistance precisely located on their respective sides of the transformer. Because it

In press

preserves the actual configuration, the exact equivalent circuit provides the most accurate representation of transformer behaviour under steady-state conditions. It is typically used when high analytical precision is required, such as in performance evaluation, loss calculations, and detailed design studies.

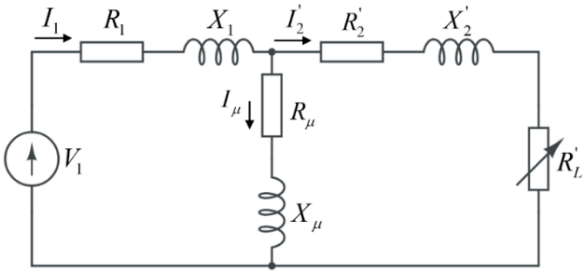

Fig. 2. Exact steady-state equivalent circuit of single-phase transformers

Where:

- R_1: Primary winding resistance
- R_2': Secondary winding resistance referred to the primary winding
- X_1: Leakage reactance of the primary winding
- X_2': Leakage reactance of the secondary winding referred to the primary winding
- R_μ: Core loss resistance
- X_μ: Magnetizing reactance
- R_L': Load resistance referred to the primary winding
- I_1: Primary current
- I_μ: Magnetizing current
- I_2': Secondary current referred to the primary winding

The approximate steady-state equivalent circuit of a single-phase transformer is shown in Fig. 3. This simplified model is derived from the exact circuit by transferring impedances from one side of the transformer to the other using the square of the turns ratio. Certain elements-usually those that contribute minimally to the overall behavior-may be neglected or combined to streamline analysis. Although slightly less accurate than the exact model, the approximate equivalent circuit is much easier to use and sufficiently precise for most engineering calculations, including voltage regulation, efficiency estimation, and routine system studies. The circuit is particularly useful for applying optimization techniques, such as the Nelder-Mead method, to accurately estimate the parameters of the exact equivalent circuit. It provides suitable initial conditions that improve both the precision and convergence of iterative parameter estimation.

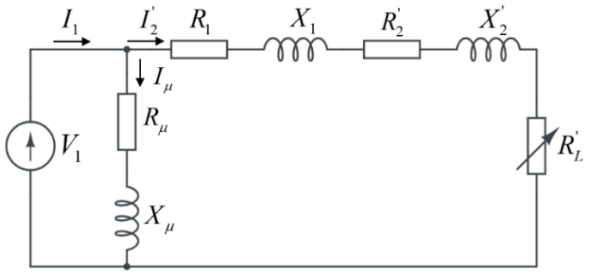

Fig. 3. Approximate steady-state equivalent circuit of single-phase transformers

Based on the approximate steady-state equivalent circuit of a single-phase transformer, the following parameters can be conveniently calculated using the no-load test:

Core loss resistance:

$$R_\mu = \frac{P_1}{I_1^2} \tag{12}$$

Magnetizing impedance:

$$|Z_\mu| = \frac{V_1}{I_1} \tag{13}$$

Magnetizing reactance:

$$X_\mu = \sqrt{|Z_\mu|^2 - R_\mu^2} \tag{14}$$

Where:

- V_1: Measured RMS voltage of the primary winding
- I_1: Measured RMS current of the primary winding
- P_1: Measured real power of the primary winding

By performing the load test, the parameters of the primary and secondary windings can be determined as follows:

$$\dot{I}_2 = \dot{I}_1 - \dot{I}_\mu = \dot{I}_1 - \frac{\dot{V}_1}{R_\mu + jX_\mu} \tag{15}$$

$$Z_2' = \frac{\dot{V}_1}{\dot{I}_2} = \left(R_1 + R_2' + R_L'\right) + j\left(X_1 + X_2'\right) \tag{16}$$

R_1 and R_2' can be computed as follows:

$$R_1 = R_2' = \frac{Real(Z_2') - R_L'}{2} \tag{17}$$

X_1 and X_2' can be calculated as follows:

In press

$$X_1 = X_2^{'} = \frac{Imag(Z_2^{'})}{2} \tag{18}$$

The values of R_μ, X_μ, R_1, X_1, $R_2^{'}$ and $X_2^{'}$ will be utilized to precisely determine the parameters of the exact equivalent circuit of the transformer as shown in Fig. 2 with the use of the Nelder-Mead method.

4. Bayesian Neural Networks for Regression

BNNs can be seen as an extension version of feedforward neural networks (FNNs) that incorporate Bayesian inference to handle uncertainty in network parameters including weights and biases. Instead of assigning fixed values to weights and biases, BNNs treat them as probability distributions, allowing the network to make probabilistic predictions. In Bayesian framework for FNNs, the distribution of weights and biases in an FNN before and after training can be assumed to Gaussian distribution. Applying Bayes rule gives the posterior distribution of the weights and biases as follows:

$$p(w|D) = \frac{p(D|w)\,p(w)}{p(D)} \tag{19}$$

Where:

- $p(w|D)$: Posterior distribution of the weights and biases after the network is trained.
- $p(D|w)$: Likelihood function, which contains information about the weights and biases from observations.
- $p(w)$: Prior distribution of the weights and biases contains information about the weights and biases from background knowledge.
- $p(D)$: Evidence for the network.

Based on Bayesian inference for FNNs, the regularization parameters in a cost function can be conveniently estimated. A BNN usually consists of three layers as follows:

- Input layer receives the input data (features).
- Hidden layer performs computations and extracts relationships or patterns.
- Output layer produces the result or decision.

4.1. Forward Propagation

The input values to the network are denoted by x_i where $i = 1,...,d$. The activation of the hidden layer is as follows:

$$a_j^{(1)} = \sum_{i=1}^{d} w_{ji}^{(1)} x_i + b_j^{(1)} \qquad j = 1,...,M \tag{20}$$

Where:

- $w_{ji}^{(1)}$: Weight on the connection from the i-th input to the j-th hidden node
- $b_j^{(1)}$: Bias of the j-th hidden node
- $a_j^{(1)}$: Activation of the j-th hidden node
- d: Number of inputs
- M: Number of hidden nodes

The activations of the hidden layer are then used to compute the outputs of hidden nodes as follows:

$$y_j^{(1)} = f_1\left(a_j^{(1)}\right) \tag{21}$$

Where $f_1(\cdot)$ is the activation function of the hidden nodes, which is a 'tanh' function as follows:

$$y_j^{(1)} = \tanh\left(a_j^{(1)}\right) \tag{22}$$

The activation function of the hidden nodes has the following properties:

$$\frac{\partial y_j}{\partial a_j} = 1 - y_j^2 \tag{23}$$

Equation (23) is used for backpropagation during the network training process.

The activations of output nodes are computed as follows:

$$a_k^{(2)} = \sum_{j=1}^{M} w_{kj}^{(2)} y_j + b_k^{(2)} \qquad k = 1,...,c \tag{24}$$

Where:

- $w_{kj}^{(2)}$: Weight on the connection from the j-th hidden node to the k-th output node
- $b_k^{(2)}$: Bias of the k-th output node
- $a_k^{(2)}$: Activation of the k-th output node
- c: Number of output nodes

For regression problems, the linear function is used for the activation of the output nodes, which is as follows:

$$z_k = a_k^{(2)} \tag{25}$$

4.2. Cost Function

The training of the BNN requires defining a cost function, which has the following form:

$$S = \beta E_D + \alpha E_W \tag{26}$$

Where E_D is the sum-of-square error function as follows:

$$E_D = \frac{1}{2}\sum_{n=1}^{N}\sum_{k=1}^{c}\left\{z_k\left(x_n; w\right) - t_{nk}\right\}^2 \tag{27}$$

Where:

- x_n: The n-th input data

In press

- t_n : The n -th target data corresponding to the k -th output
- w : Vector of weights and biases
- N : Number of patterns in the training data

E_D is also known as the data error function. E_W is called the weight function, which is given by:

$$E_W = \frac{1}{2}\|w\|^2 = \sum_{i=1}^{W} w_i^2 \tag{28}$$

Where W is the number of weights and biases in the network. β represents the constant inverse variance and α denotes the regularization constant that penalizes large weights and biases, thereby mitigating the overfitting phenomenon in the network after training.

Under Bayesian inference, at the most probable vector of weights and biases, w_{MP}, the relationship between E_W^{MP} and α is as follows:

$$2\alpha E_W^{MP} = W - \sum_{i=1}^{W} \frac{\alpha}{\lambda_i + \alpha} \tag{29}$$

In which $\lambda_i \left(i = 1,...,W\right)$ are the eigenvalues of the Hessian matrix (second-order derivative matrix) of the data error function, E_D. The right-hand side of (29) is equal to a value γ defined as follows:

$$\gamma = \sum_{i=1}^{W} \frac{\lambda_i}{\lambda_i + \alpha} \tag{30}$$

From (29) and (30), the value of α can be computed as follows:

$$\alpha = \frac{\gamma}{2E_W^{MP}} \tag{31}$$

At the most probable vector of weights and biases, w_{MP}, the relationship between E_D^{MP} and β is as follows:

$$\beta = \frac{N - \gamma}{2E_W^{MP}} \tag{32}$$

Equations (30), (31) and (32) are used to update the values of α and β during the network training process.

4.3. Network Training

BNN training is carried out by iteratively updating the weight and bias vectors as follows:

$$w_{k+1} = w_k + \eta_k d_k \tag{33}$$

Where:

- w_k : Vector of weights and biases at the k-th iteration
- w_{k+1} : Vector of weights and biases at the k+1-th iteration
- d_k : Search direction at the k-th iteration
- η_k : Learning rate at the k-th iteration

The vector of weights and biases is updated using a method called backpropagation and the network training procedure includes the following steps:

- **Step 1:** Choose initial values for the hyperparameters α and β. Initialize the weights and biases in the network.
- **Step 2:** Train the network with the scaled conjugate gradient algorithm to minimize the cost function, S.
- **Step 3:** When the network training has reached a local minimum, the values of α and β can be re-estimated as follows:

$$\alpha_{new} = \frac{\gamma_{old}}{2E_W} \tag{34}$$

$$\beta_{new} = \frac{N - \gamma_{old}}{2E_W} \tag{35}$$

- **Step 4:** Repeat Steps 2 and 3 until convergence.

5. The Nelder-Mead Method

The Nelder-Mead method, also known as the downhill simplex method, is a derivative-free optimization algorithm used to find a local minimum (or maximum) of a function in a multidimensional space. The method is very useful when:

- The objective function is nonlinear, noisy, or discontinuous.
- Derivatives (gradients) are not available or difficult to compute.

Instead of using gradients, the Nelder-Mead method is based on a simplex, which is a geometric fig with $n+1$ vertices in an n-dimensional space. The algorithm moves and reshapes the simplex iteratively to approach a minimum of the objective function. The Nelder-Mead algorithm includes the following steps:

In this study, the Nelder–Mead method is used to estimate the parameters of the exact equivalent circuit of an existing single-phase transformer. The parameters of the approximate equivalent circuit, together with the measured electrical data from the no-load and load tests, serve as initial conditions for the optimization process. This enables accurate determination of the parameters of the exact equivalent circuit.

In press

Let $f(x)$ be the objective function to minimize.

1) **Initialize the simplex:**
   Choose $n+1$ initial points $x_1, x_2, ..., x_{n+1}$.
2) **Order:**
   Evaluate $f(x_i)$ at each vertex and order them:
   $f(x_1) \le f(x_2) \le ... \le f(x_{n+1})$.
3) **Compute the centroid:**
   $x_c = \frac{1}{n}\sum_{i=1}^{n} x_i$ (exclude the worst point x_{n+1}).
4) **Reflection:**
   Reflect the worst point through the centroid:
   $x_r = x_c + \alpha(x_c - x_{n+1})$, where $\alpha \approx 1$.
   - If $f(x_1) \le f(x_r) < f(x_n)$, accept x_r and replace x_{n+1}.
5) **Expansion:**
   If $f(x_r) < f(x_1)$, try expanding further:
   $x_e = x_c + \gamma(x_r - x_c)$, where $\gamma = 2$.
   Accept x_e if it improves further.
6) **Contraction:**
   If $f(x_r) > f(x_n)$, try a contraction:
   $x_c^{'} = x_c + \rho(x_{n+1} - x_c)$, where $\rho \approx 0.5$.
7) **Shrink:**
   If contraction fails, shrink all points toward the best point x_1:
   $x_i = x_1 + \sigma(x_i - x_1)$, where $\sigma = 0.5$.
8) **Repeat** until convergence (small change in function value or simplex size).

6. Design of Single-Phase Transformers Using Bayesian Neural Networks

The design of single-phase power transformers using BNNs requires generating an appropriate training dataset. A FEA model was developed to design single-phase power transformers.

The inputs parameters of the FEA model are as follows:

- Primary voltage: $V_1 = 220(V)$
- Secondary voltage: $V_2 = 110(V)$
- Frequency: $f = 50(Hz)$
- Maximum flux density: $B(T)_{max}$
- Maximum current density: $J = 2.5(A/mm^2)$
- Fill factor: $k_w = 0.4$

The output parameters of the FEA model include:

- Dimensional parameters: w_1, w_2 and d
- Number of turns in the primary winding: N_1
- Number of turns in the secondary winding: N_2

When the secondary winding is connected to a load, the FEA model can also compute the following parameters:

- Current in the primary winding: I_1
- Current in the secondary winding: I_2

Fig. 4 illustrates the magnetic flux distribution in a single-phase power transformer, as obtained from the use of FEMM. The visualization provides insight into the core's magnetic behaviour, highlighting regions of high flux density.

The dataset used to train the BNN was formed by using the FEA model with the input parameters as follows:

- Primary voltage: $V_1 = 220(V)$
- Secondary voltage: $V_2 = 110(V)$
- Maximum input power: $P_{1,\max} = 100(W)$
- Load resistance: $R_L = 100 \div 700(\Omega)$

The outputs of the FEA model are as follows:

- Dimensional parameters: w_1, w_2 and d
- Number of turns in the primary winding: N_1
- Number of turns in the secondary winding: N_2

Fig. 5 illustrates the principle for generating the dataset, which is carried out using FEMM. The BNN has the following architecture:

- Three inputs corresponding to the rated voltages of the primary and secondary windings, and the maximum input power (V_1, V_2 and $P_{1,\max}$)
- Ten nodes in the hidden layer (can be varied)
- Five outputs corresponding to five design parameters (w_1, w_2, d, N_1 and N_2)

Fig. 6 illustrates the complete training procedure of the BNN model. During this process, the network's weights and biases are iteratively adjusted using the scaled conjugate gradient (SCG) algorithm, which efficiently minimizes the predefined cost function. By progressively reducing the prediction error, the SCG optimizer enables the BNN to learn the underlying relationship between the input features and the desired output, thereby ensuring a more accurate and reliable parameter mapping.

Table 1 shows the variation of hyperparameters over five successive re-estimation periods, illustrating how the network adapts and refines its predictions throughout the training process. This iterative adjustment of both weights and hyperparameters improves the network's ability to generalize, reduces overfitting, and enhances the overall reliability of the model.

In press

Table 1. Changes in the hyperparameters over the re-estimation periods

Re-estimation periods	α	β
1	3.079012	31361.14
2	2.989626	33033.44
3	3.061648	32504.52
4	2.951501	33359.24
5	2.885049	33878.68

Table 2 presents the transformer design parameters, which were determined based on the nominal primary and secondary voltages, as well as the maximum input power rating. These parameters define both the physical and electrical characteristics of the transformer. Specifically, they include elements such as the core dimensions, the number of turns in each winding, wire gauges, and core material selection. These values directly influence the transformer's magnetic performance, voltage transformation capability, and thermal behavior during operation. In addition, the parameters serve as a foundation for estimating key performance indices such as efficiency, voltage regulation, and losses.

Table 3 summarizes the electrical parameters of the designed single-phase power transformer after completing the design stage. These parameters were evaluated under a range of loading conditions to assess the transformer's operational behavior. The table includes values such as winding resistances, leakage reactance, magnetizing inductance, and core loss components, which were obtained using the proposed modelling and parameter extraction methods. The results help validate the accuracy of the design, verify compliance with performance requirements, and demonstrate the effectiveness of the proposed BNN-based design approach.

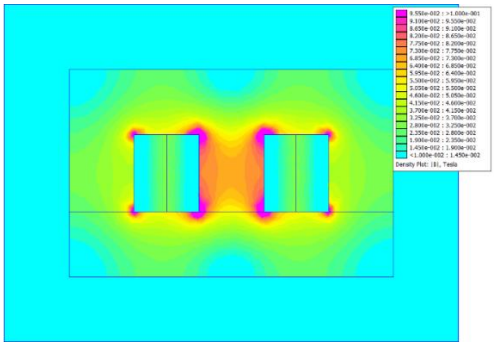

Fig. 4. 2D FEM analysis of a single-phase power transformer

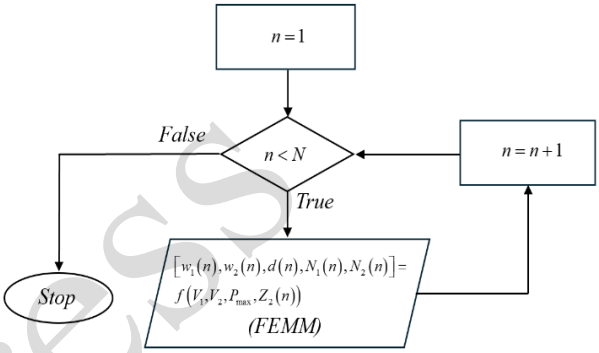

Fig. 5. Principle for generating the dataset

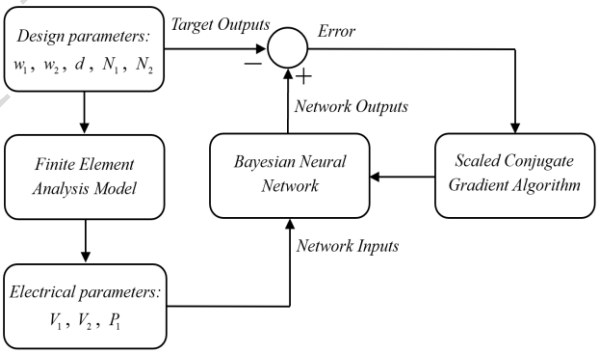

Fig. 6. Principle for training the BNN

Table 2. Design parameters of the single-phase power transformer are determined according to the maximum input power

$R_L\,(\Omega)$	$P_{1,\max}\,(W)$	$w_1\,(mm)$	$w_2\,(mm)$	$d\,(mm)$	$N_1\,(turns)$	$N_2\,(turns)$
200	60.5000	47	70	23	6590	3275
300	40.3333	46	51	23	6598	3290
400	30.2500	44	40	22	6601	3295
500	24.2000	43	34	21	6603	3297
600	20.1667	41	30	20	6604	3298
700	17.2857	40	26	20	6604	3299

In press

Table 3. Electrical parameters of the single-phase power transformer after design corresponding to different load schemes

$R_L(\Omega)$	$V_1(V)$	$I_1(A)$	$V_2(V)$	$I_2(A)$	$P_1(W)$
200	220.0780	0.2616	105.2375	0.5260	57.5831
300	219.9512	0.1770	106.3374	0.3545	38.9293
400	220.0879	0.1339	107.1758	0.2678	29.4637
500	220.0787	0.1077	107.6860	0.2153	23.6954
600	220.0577	0.0901	108.1031	0.1801	19.8300
700	220.0513	0.0774	108.2038	0.1545	17.0214

To demonstrate the effectiveness of the proposed transformer design method, a laboratory single-phase transformer manufactured by Lab-Volt is redesigned using the following electrical parameters:

- The nominal primary voltage: $V_1 = 220(V)$
- The nominal secondary voltage: $V_2 = 110(V)$
- The primary current: $I_1 = 0.24(A)$

Using the trained BNN to design the transformer provides the design and electrical parameters, as shown in Tables 4 and 5, respectively. In Table 5, η represents the efficiency of the transformer.

Table 4. Design parameters of the single-phase power transformer obtained from the trained BNN

$w_1(mm)$	$w_2(mm)$	$d(mm)$	$N_1(turns)$	$N_2(turns)$
54	60	27	6607	3303

Table 5. Electrical parameters of the single-phase power transformer obtained from the FEA model

$V_1(V)$	$I_1(A)$	$V_2(V)$	$S(VA)$	$\eta(\%)$
219.9744	0.246	103.2460	54.1270	0.9379

The electrical parameters of the transformer represent its operating point and will later be used to compare the designed model with the measured parameters of an actual power transformer in the next section.

7. Experimental Validation

An experimental system for condition monitoring of a single-phase transformer is shown in Fig. 7, which includes the following components:

- A single-phase transformer manufactured by Lab-Volt (55 VA, 220 V; 0.25 A, 50 Hz)
- A measurement board equipped with AC voltage and current sensors
- An NI USB-6009 data acquisition device (DAQ) from National Instruments, with a sampling rate of 10 kHz

Fig. 8 shows the graphical user interface (GUI) of the DAQ software, which provides the following functions:

- Display the waveforms of the primary voltage and current
- Display the RMS values of the primary voltage and current
- Display the total harmonic distortion (THD) of the primary voltage
- Display the THD of the primary current
- Display the harmonic amplitudes of the primary current
- Save the data for offline analyses

Table 6 presents the measured RMS values of the primary and secondary voltages, along with the corresponding input power. These experimental measurements serve as essential inputs for estimating the parameters of both the approximate and exact equivalent circuits of the transformer. Accurate determination of these parameters is crucial for assessing the transformer's performance-such as voltage regulation, efficiency, and loss characteristics-and for validating the effectiveness of the proposed design and modelling approach.

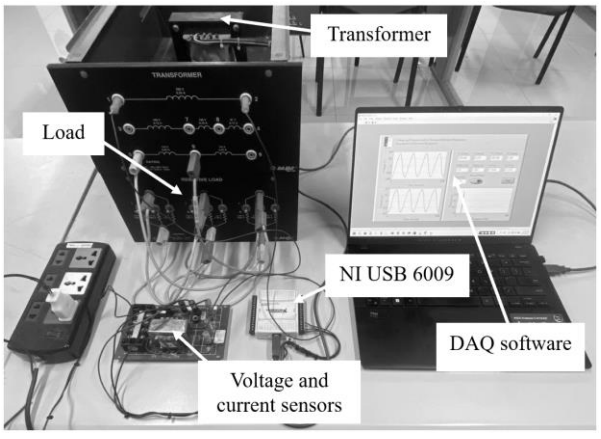

Fig. 7. The experimental system

In press

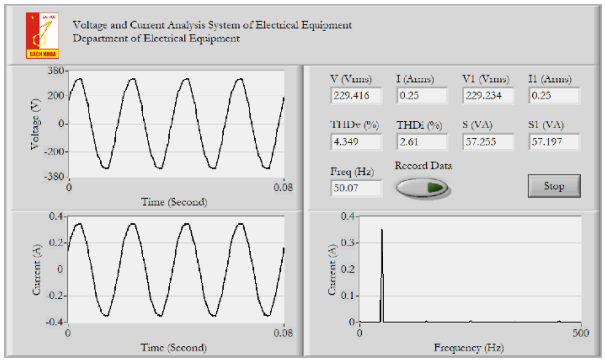

Fig. 8. GUI of the DAQ software

Table 6. Electrical parameters of the single-phase power transformer obtained from the FEA model

Condition	$V_1(V)$	$I_1(A)$	$P_1(W)$
No-load	231.5521	0.0125	1.7471
$R_L = 210(\Omega)$	227.2545	0.2374	53.2186

The magnetizing resistance and reactance can be initially determined from the no-load test for the approximate equivalent circuit as follows:

$$R_\mu = \frac{P_1}{I_1^2};\ Z_\mu = \frac{V_1}{I_1};\ X_\mu = \sqrt{Z_\mu^2 - R_\mu^2} \tag{36}$$

Based on the load test with the approximate equivalent circuit, the magnetizing current is determined as follows:

$$\dot{I}_\mu = \frac{\dot{V}_1}{R_\mu + jX_\mu} \tag{37}$$

At a load test, the input resistance of the approximate equivalent circuit is computed as follows:

$$R_{in} = \frac{P_1}{I_1^2} \tag{38}$$

The input impedance of the approximate equivalent circuit is calculated as follows:

$$Z_{in} = \frac{V_1}{I_1} \tag{39}$$

The input reactance of the approximate equivalent circuit is given by:

$$X_{in} = \sqrt{Z_{in}^2 - R_{in}^2} \tag{40}$$

The input current of the approximate equivalent circuit is given by:

$$\dot{I}_1 = \frac{\dot{V}_1}{R_{in} + jX_{in}} \tag{41}$$

The currents in the primary and secondary winding computed as follows:

$$\dot{I}_2 = \dot{I}_1 - \dot{I}_\mu \tag{42}$$

The values of R_1 and $R_2^{'}$ are determined as follows:

$$R_1 = R_2^{'} = \frac{1}{2}\left[Real\left(\frac{\dot{V}_1}{\dot{I}_2}\right) - k^2 R_L \right] \tag{43}$$

In which $k = V_1 / V_2 = 2$ and is also known as the voltage transformation ratio. The values of X_1 and $X_2^{'}$ are computed as follows:

$$X_1 = X_2^{'} = \frac{1}{2} Imag\left(\frac{\dot{V}_1}{\dot{I}_2}\right) \tag{44}$$

The parameters of the approximate equivalent circuit are then used as initial values to estimate the parameters of the exact equivalent circuit of the transformer using the Nelder-Mead method. To obtain the parameters of the exact equivalent circuit, a cost function first needs to be formed by following the steps below:

$$Z_1 = R_1 + jX_1 \tag{45}$$

$$Z_\mu = R_\mu + jX_\mu \tag{46}$$

$$Z_2 = \left(R_2^{'} + k^2 R_L\right) + jX_2^{'} \tag{47}$$

The input impedance of the exact equivalent circuit is given by:

$$Z_{in} = Z_1 + \frac{Z_\mu Z_2}{Z_\mu + Z_2} \tag{48}$$

The input resistance of the exact equivalent circuit is computed as follows:

$$R_{in} = Real\left(Z_{in}\right) \tag{49}$$

The input reactance of the exact equivalent circuit is computed as follows:

$$X_{in} = Imag\left(Z_{in}\right) \tag{50}$$

A cost function is then defined as follows:

$$J = \left|R_{in} - R_{in}^{meas}\right| + \left|X_{in} - X_{in}^{meas}\right| \tag{51}$$

Where:

- R_{in}^{meas}: Measured input resistance of the transformer
- X_{in}^{meas}: Measured input reactance of the transformer

The Nelder-Mead method is employed to minimize the defined cost function. Table 7 presents the optimization progress by listing the parameter values obtained during the first ten iterations of the

In press

Nelder-Mead algorithm. Once the optimization process is completed, the parameters of the transformer's exact equivalent circuit are determined.

Table 7. Optimization parameters during the first ten iterations of the Nelder-Mead method

Iteration	Function-Count	min f(x)	Procedure
0	1	20.8483	
1	7	20.8483	initial
2	9	16.8137	expand
3	10	16.8137	reflect
4	11	16.8137	reflect
5	13	14.7381	expand
6	14	14.7381	reflect
7	16	6.23724	expand
8	17	6.23724	reflect
9	18	6.23724	reflect
10	19	6.23724	reflect

Table 8 summarizes these exact equivalent circuit parameters before and after optimization. In addition, Table 9 reports the measured electrical parameters of the transformer under different load resistances, while Table 10 provides the design parameters corresponding to various values of the maximum input power.

Table 11 presents a side-by-side comparison between the simulated and measured electrical parameters of the transformer. The close agreement between these results confirms that the design parameters derived from the proposed methodology accurately represent the behaviour of the actual single-phase power transformer. The simulated values closely match the measured RMS voltages, currents, and input power, indicating that the estimated equivalent-circuit parameters reliably capture the electrical characteristics of the transformer. This strong correlation validates both the modelling approach and the optimization procedure, demonstrating their suitability for accurate transformer design, analysis, and performance evaluation.

Table 8. Optimization parameters during the first ten iterations of the Nelder-Mead method

	$R_m(\Omega)$	$X_m(\Omega)$	$R_1(\Omega)$	$X_1(\Omega)$	$R_2'(\Omega)$	$X_2'(\Omega)$
Before optimization	11173	14767	70.1917	63.3735	70.1917	63.3735
After optimization	11821	15204	62.8214	64.0460	67.1319	64.9518

Table 9. Measured operating parameters of the transformer under different load resistances

$R_L(\Omega)$	$V_1(V)$	$I_1(A)$	$P(W)$	$S(VA)$	PF
210	227.2545	0.2374	53.2186	53.9480	0.9865
314	228.4764	0.1687	38.1263	38.5450	0.9891
630	228.0481	0.0920	20.7110	20.9709	0.9876

Table 10. Design parameters of the transformer under different load levels

$R_L(\Omega)$	$P_{1,\max}(W)$	$w_1(mm)$	$w_2(mm)$	$d(mm)$	$N_1(turns)$	$N_2(turns)$
210	54.9540	47	67	23	6591	3343
314	38.5350	46	49	23	6599	3291
630	19.2063	41	28	20	6604	3298

Table 11. Comparison of the electrical parameters of the transformer obtained by simulation and measurement

	$R_L=210(\Omega)$		$R_L=314(\Omega)$		$R_L=630(\Omega)$	
	Simulation	Experiment	Simulation	Experiment	Simulation	Experiment
$V_1(V)$	220.0559	227.2545	220.0732	228.0481	219.9487	228.0481
$I_1(A)$	0.2497	0.2374	0.1699	0.1687	0.0858	0.0920
$P(W)$	54.9540	53.2186	37.3947	38.1263	18.8787	20.7110
$S(VA)$	54.9540	54.5819	37.3947	38.5450	18.8787	20.9709

8. Conclusion

This study demonstrates that combining BNNs with FEM simulations offers a highly efficient, accurate, and intelligent framework for designing single-phase transformers. In the proposed approach, the BNN learns directly from datasets generated by FEM analyses, enabling it to capture complex and nonlinear relationships between the transformer's geometric features, electrical parameters, and overall performance indicators. By leveraging these data-driven insights, the model delivers precise predictions of key electrical

In press

characteristics while drastically reducing computation time when compared to conventional analytical calculations or empirical design procedures.

The results show a strong correlation among FEM simulation outputs, BNN-based predictions, and laboratory measurements, validating the robustness, reliability, and physical consistency of the approach. In addition, the flexibility of the methodology allows it to be easily adapted for various transformer configurations and extended to other electromagnetic devices such as motors, inductors, and power converters. Overall, this hybrid framework effectively bridges physics-based modelling and machine-learning intelligence, paving the way for faster, more accurate, and automated transformer design processes suitable for both academic research and industrial engineering applications.

Acknowledgments

This research is funded by Hanoi University of Science and Technology (HUST) under project number T2024-PC-059.

References

[1] Q. Peng, H. Du, Z. Zheng, H. Zhu, and Y. Fang, Prediction of magnetic fields in single-phase transformers under excitation inrush based on machine learning, Sensors, vol. 25, no. 13, Art. no. 4150, 2025. https://doi.org/10.3390/s25134150

[2] N. Schwartze, S. Moschik, and M. Reichhartinger, Evaluation of a control-oriented single-phase transformer core model, COMPEL, vol. 44, no. 5, pp. 784–800, 2025. https://doi.org/10.1108/COMPEL-01-2025-0014

[3] B. A. Luciano, M. E. Morais, and C. S. Kiminami, Single phase 1-kVA amorphous core transformer: Design, experimental tests, and performance after annealing, IEEE Trans. Magn., vol. 35, no. 4, pp. 2152–2154, 1999. https://doi.org/10.1109/20.774186

[4] S. Sorte, A. F. Monteiro, D. Ventura, A. Salgado, M. S. A. Oliveira, and N. Martin, Power transformers cooling design: A comprehensive review, Energies, vol. 18, Art. no. 1051, 2025. https://doi.org/10.3390/en18051051.

[5] S. Kul and T. Sulayman, Comparison of FEA-based thermal and loss analyses of the dry-type transformer using different grades of core material, Electrica, vol. 23, 2022. https://doi.org/10.5152/electrica.2022.22003

[6] A. Ferreira, P. Picher, F. Meghnefi, I. Fofana, H. Ezzaidi, C. Volat, and V. Behjat, Reproducing transformers' frequency response from finite element method (FEM) simulation and parameters optimization, Energies, vol. 16, 2023, Art. no. 4364. https://doi.org/10.3390/en16114364

[7] S. Muhammad, S. Abdulrazak, G. A. Bakare, S. Abdulhafiz, and M. Danladi, Modelling and analysis of a power transformer using finite element analysis, Asian Journal of Science Technology Engineering and Art, vol. 3, pp. 902–920, 2025. https://doi.org/10.58578/ajstea.v3i3.5703

[8] R. Kazemi, S. Jazebi, D. Deswal, and D. L. Francisco, Estimation of design parameters of single-phase distribution transformers from terminal measurements, IEEE Trans. Power Del., pp. 2031–2039, 2017. https://doi.org/10.1109/TPWRD.2016.2621753

[9] M. P. Calasan, A. Jovanovic, V. Rubezic, D. Mujicic, and A. Deriszadeh, Notes on parameter estimation for single-phase transformer, IEEE Trans. Ind. Appl., vol. 56, no. 4, pp. 3710–3718. 2020. https://doi.org/10.1109/TIA.2020.2992667

[10] D. Bhowmick, M. Manna, and S. Chowdhury, Estimation of equivalent circuit parameters of transformer and induction motor from load data, IEEE Trans. Ind. Appl., vol. 54, no. 3, pp. 2784–2791, 2018. https://doi.org/10.1109/TIA.2018.2790378

[11] M. Nazmunnahar, S. Simizu, P. R. Ohodnicki, S. Bhattacharya, and M. E. McHenry, Finite-element analysis modeling of high-frequency single-phase transformers enabled by metal amorphous nanocomposites and calculation of leakage inductance for different winding topologies, IEEE Trans. Magn., vol. 55, no. 7, 2019. https://doi.org/10.1109/TMAG.2019.2904007

[12] T. N. Son, P. M. Tu, H. Anh, T. C. Trung, V. L. Tinh, and Q. H. Hoang, Fast and accurate inductor design using feedforward neural networks trained by Quasi-Newton method, in Proc. Int. Conf. Adv. Mach. Learn. Data Sci. (AMLDS), Jul. 2025. https://doi.org/10.1109/AMLDS63918.2025.11159454

[13] B. Poudel and E. Amiri, Deep learning based design methodology for electric machines: Data acquisition, training and optimization, IEEE Access, vol. 11, pp. 18281–18290, 2023. https://doi.org/10.1109/ACCESS.2023.3247011

[14] I. T. Nabney, Netlab: Algorithms for pattern recognition. New York, NY, USA: Springer, 2002.

In press